

1 **Multi-hazard fragility analysis for fluvial dikes in earthquake and** 2 **flood prone areas**

3 Sergey Tyagunov¹, Sergiy Vorogushyn², Cristina Muñoz Jimenez¹, Stefano Parolai^{1*},
4 Kevin Fleming¹

5 (1) GFZ German Research Centre for Geosciences, Centre for Early Warning,
6 Helmholtzstrasse 7, D-14467, Potsdam, Germany.

7 (2) GFZ German Research Centre for Geosciences, Section 5.4 Hydrology,
8 Telegrafenberg, D-14473, Potsdam, Germany.

9 *now at: Seismological Research Centre of the OGS Istituto Nazionale di
10 Oceanografia e di Geofisica Sperimentale, Borgo Grotta Gigante 42/C, 34010 Sgonico,
11 Italy.

12 Correspondence to: Sergey Tyagunov, sergey.tyagunov@gmail.com

13 Keywords: multi-hazard; fragility; liquefaction; dike failure probability; earthquake;
14 flood; Rhine; Cologne

15

16 **Abstract**

17 The paper presents a methodology for multi-hazard fragility analysis for fluvial
18 earthen dikes in earthquake and flood prone areas due to liquefaction. The
19 methodology has been applied for the area along the Rhine River reach and
20 adjacent floodplains between the gauges Andernach and Düsseldorf. Along this
21 domain, the urban areas are partly protected by dikes, which may be prone to failure
22 during exceptional floods and/or earthquakes. The fragility of the earthen dikes is
23 analyzed in terms of liquefaction potential characterized by the factor of safety
24 estimated with the use of the procedure of Seed and Idriss (1971). Uncertainties in
25 the geometrical and geotechnical dike parameters are considered in a Monte Carlo
26 simulation (MCS). Failure probability of the earthen structures is presented in the
27 form of a fragility surface s as a function of both seismic hazard and
28 hydrological/hydraulic load.

29

30 **Introduction**

31 Risk assessment in areas affected by several natural perils can be carried out in two
32 possible ways: on the one hand, one can consider different types of hazards and
33 risks independently, while on the other, possible interactions between hazards can
34 be taken into account. The former approach is based on traditional methods of
35 single-type hazard and risk assessment and represents a common practice. The
36 latter is used much more rarely, as it involves scenarios with obviously lower

37 occurrence probabilities, which might, therefore, be underrated and sometimes
38 unreasonably neglected. At the same time, the tragic lessons of past disasters show
39 that in multi-hazard prone areas the risk of losses from single hazardous events can
40 dramatically increase due to possible interactions between different types of hazards
41 and the occurrence of cascading effects. For instance, the devastating experience of
42 the Katrina Hurricane, 2005, and the Tohoku earthquake, 2011, sorely demonstrated
43 that low occurrence probability events may result in extremely high consequences.
44 Therefore, the possible interactions between hazards in multi-hazard prone areas
45 should not be ignored in decision making.

46 The earlier multi-hazard studies were solely based on the comparison of single-type
47 hazard and risk assessments without considering interactions and potential
48 cascading effects (e.g., HAZUS-MH, 2003, KATARISK, 2003, Grünthal et al., 2006,
49 Fleming et al., 2016). In the recent years, frameworks for the assessment of the
50 interactions of multiple hazards have been developed (e.g., Marzocchi et al., 2012,
51 Selva, 2013, Mignan et al., 2014).

52 The present research work, which was undertaken as part of the multi-hazard
53 (earthquake-flood) risk study implemented in the frame of the EU FP7 project
54 MATRIX (New Multi-Hazard and Multi-Risk Assessment Methods for Europe)
55 focuses on the problem of multi-hazard fragility analysis of fluvial earthen levee. We
56 develop the methodology for assessment of fragility due to liquefaction by taking into
57 account potential flood and earthquake impacts on dikes at the Rhine reach around
58 Cologne.

59 The middle Rhine is regularly affected by flooding (e.g., Fink et al., 1996) and vast
60 floodplains are protected by dikes. The areas not protected by dikes are typically
61 behind concrete walls, protected by mobile flood protection walls or are located on
62 elevated banks.

63 Besides flood hazard, the areas around Cologne are exposed to other types of
64 natural hazards, in particular windstorms (e.g., Hofherr and Kunz, 2010) and
65 earthquakes (Grünthal et al., 2009, Fleming et al., 2016). Although rarer than floods
66 or windstorms, earthquakes have a higher damage potential (Grünthal et al., 2006,
67 Fleming et al., 2016). In combination with high water levels, earthquake may lead to
68 liquefaction of saturated earthen dikes.

69 Dikes may fail due to various failure mechanisms induced either by high water levels
70 and/or earthquake impact (Armbruster-Veneti, 1999, Foster et al., 2000, Apel et al.,
71 2004, Allsop et al., 2007, Briaud et al., 2008, Wolff, 2008, Van Baars and Van
72 Kempen, 2009, Vorogushyn et al., 2009, Nagy, 2012, Huang et al., 2014). When
73 considering solely hydrologic/hydraulic load, overtopping is the most common failure
74 mechanism followed by piping and slope instability (see Vorogushyn et al., 2009 and
75 references therein). For these breach mechanisms, approaches for fragility analyses
76 has been proposed (Apel et al., 2004, Vorogushyn et al., 2009). Under earthquake

77 load, the liquefaction phenomenon is indicated as the most important cause of
78 embankment dam failure (Ozkan, 1998).

79 Marcuson et al. (2007), reviewed the development of the state of practice in seismic
80 design and analysis of embankment dams, starting from the fundamental
81 publications of Newmark (1965) and Seed and Idriss (1971). Sasaki et al. (2004)
82 described empirical and analytical methods used in Japan for estimating the
83 settlement of dikes due to liquefaction, considering both the probable subsidence of
84 the bottom boundary and deformation of the dikes. Singh and Roy (2009) proposed
85 a correlation relationship for the earthquake-induced deformation of earthen
86 embankments based on the examination of 156 published case histories and using
87 the ratio of the peak horizontal ground acceleration and the yield acceleration as an
88 estimator.

89 In recent years, more sophisticated computer-based linear or non-linear methods for
90 seismic analyses of embankments have been developed, using one-, two- (Kishida
91 et al., 2009, Athanasopoulos-Zekkos and Seed, 2013) or three-dimensional (Wang
92 et al., 2013) models. At the same time, Kishida et al. (2009) concluded that simplified
93 models based on equivalent-linear analyses can provide reasonably accurate results
94 up to moderate ground shaking levels, while nonlinear analyses should be used to
95 evaluate dike responses at stronger shaking levels. We therefore focus on a
96 simplified approach, since we are concerned with the study on a regional spatial
97 scale in the areas of low to moderate seismicity.

98 Rosidi (2007) presented a seismic risk assessment procedure for earthen
99 embankment dams and dikes, where dike fragility was expressed as a function of
100 earthquake-induced slope deformations. Considering different strengthening
101 scenarios, Rosidi (2007) estimated levee failure probabilities depending on
102 earthquake ground motion return period. However, possible fragility changes due to
103 flood water elevation and dike core soil saturation was not taken into account in that
104 study.

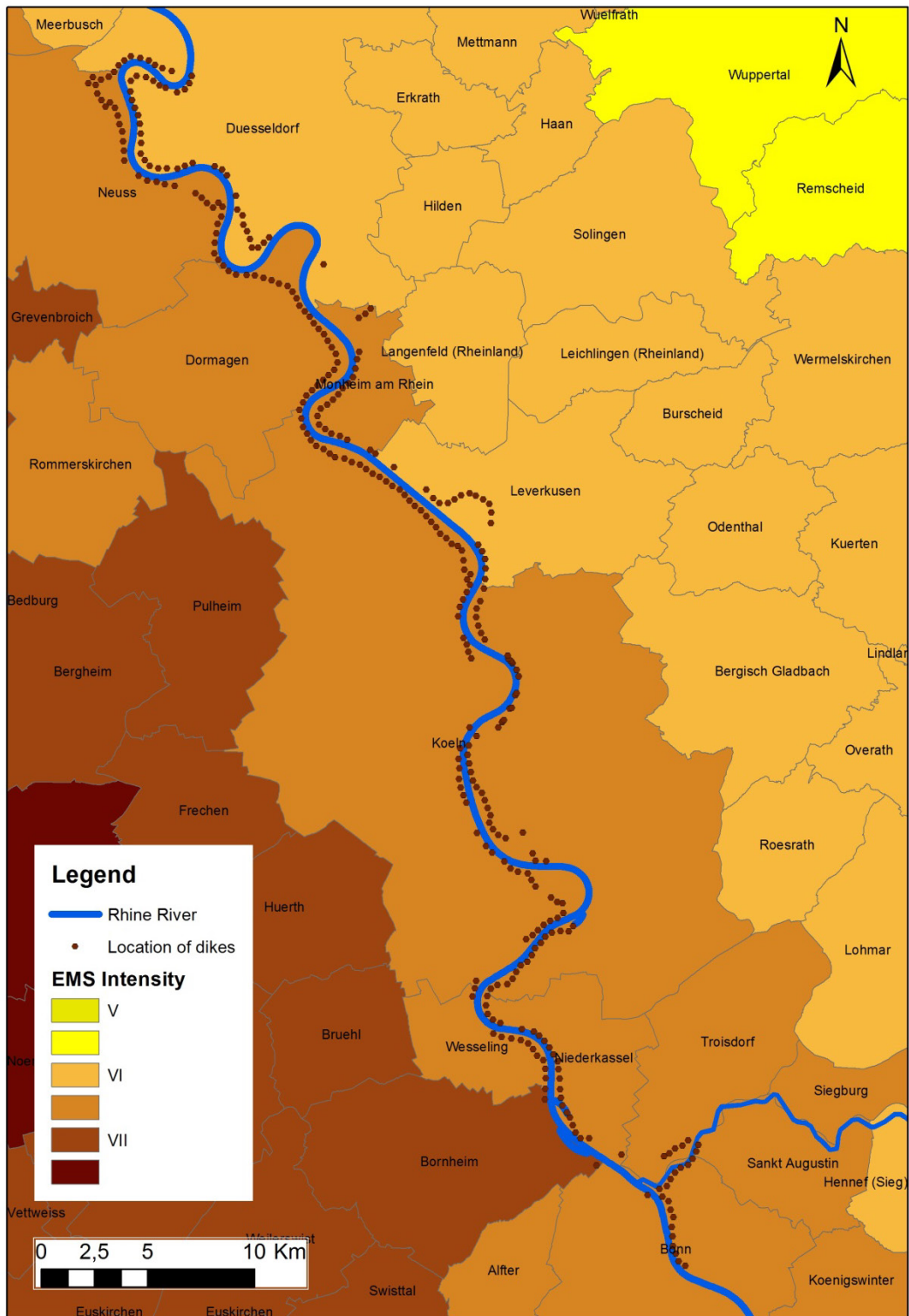
105 For the purpose of single-type flood risk assessment, Apel et al. (2004) developed
106 fragility curves for overtopping failure based on Monte Carlo simulations.
107 Vorogushyn et al. (2009) extended this approach for piping and micro-instability
108 breach mechanisms based on the formulations of Sellmeijer (1989) and
109 Vrouwenvelder & Wubs (1985), respectively.

110 Recently, Schweckendiek et al. (2014) presented an approach to include field
111 observations in the Bayesian updating of piping failure probabilities of dikes in the
112 Netherlands. Krzhizhanovskaya et al. (2011) reported an integration of reliability
113 analysis for various breach mechanisms into a prototype flood early warning system,
114 including dike failure and associated inundation modelling. A summary of research
115 and practical methods for reliability assessment of levee systems considering
116 different failure mechanisms can be found in Wolff (2008).

117 The reviewed studies, however, used a single-hazard approach focusing on either
118 earthquake or flood impacts on infrastructure. The present study aims at filling the
119 existing methodological gap considering both hazards together. The main goal of the
120 study is the development of a methodological approach for multi-hazard fragility
121 analyses and construction of multi-hazard fragility functions for dikes in the
122 earthquake and flood prone areas along the Rhine River. These functions are meant
123 to be incorporated into the regional flood hazard and risk assessment models. In this
124 way, small-scale breaching process knowledge can be integrated into regional-scale
125 risk analyses.

126 The existing regional Inundation Hazard Assessment Model IHAM (Vorogushyn et
127 al., 2010) considers three breach mechanisms: overtopping, piping and micro-
128 instability of the dike slope. More details on the parameterization of these breach
129 mechanisms and the development of respective fragility functions are given in Apel
130 et al. (2004) and Vorogushyn et al. (2009). Here we consider another possible failure
131 mechanism – earthquake-triggered physical damage to earthen dikes due to
132 liquefaction. This type of phenomena may occur in earthquake prone areas, where
133 water-saturated sandy soils have the potential to liquefy when subjected to seismic
134 vibrations. During liquefaction, when as a consequence of increased pore water
135 pressure the strength of bonds between soil particles is drastically reduced to
136 essentially zero, soil deposits may lose their bearing capacity and behave as fluids
137 (Kramer, 1996, Idriss and Boulanger, 2008). In our study, we assume that the
138 liquefaction occurrence in the dike body may result in the subsidence of the core as
139 well as in large slope deformations. The subsequent breach of the affected dike
140 section is the resulting consequence.

141 The area under study, along with the communities at risk and location of dikes along
142 the Rhine River, is presented in Fig. 1, where the points correspond to the geometric
143 centres of the dike sections of about 500-600m length. Fig.1 shows the
144 administrative boundaries (communities) as well as the general zonation of the
145 seismic hazard. The shown hazard estimates are based on the earlier map by
146 Grünthal et al. (1998) in terms of EMS intensities for an exceedance probability of
147 10% in 50 years, and are referred to the centres of communities (Tyagunov et al.,
148 2006a). The accurate seismic hazard estimates for all dikes locations will be
149 calculated below.



150

151 Figure 1: Location of flood protection dikes along the Rhine and the spatial
 152 distribution of seismic hazard in the study area in terms of EMS intensities for an
 153 exceedance probability of 10% in 50 years (Grünthal et al., 1998).

154

155 **Data and Method**

156 The probability of a dike failure is considered in terms of liquefaction potential,
 157 estimated using the method of Seed and Idriss (1971). The liquefaction potential can
 158 be assessed with a factor of safety (FS) against liquefaction, which is determined as
 159 the ratio of the capacity of the soil to resist liquefaction (CRR: Cyclic Resistance
 160 Ratio) and the seismic demand placed on the soil layer (CSR: Cyclic Stress Ratio).

161 The CSR value can be estimated using the following expression:

162

$$163 \quad CSR = 0.65 \cdot \frac{a_{max}}{g} \cdot \frac{\sigma_{vo}}{\sigma'_{vo}} \cdot r_d, \quad (1)$$

164

165 where a_{max} is the horizontal peak ground acceleration (PGA), g is the gravitational
 166 acceleration, σ_{vo} and σ'_{vo} are the total and effective overburden stresses (pressure
 167 imposed by above layers) of the soil, respectively, and r_d is a stress reduction factor
 168 that depends on the depth. For the calculation of the vertical stresses as a function
 169 of depth, we also consider the variations in the water level in the river, which
 170 influences the phreatic surface and degree of saturation in the dike core.

171 As for the CRR value, there are different methods for estimating the soil resistance
 172 to liquefaction (Youd et al., 2001, Kramer and Mayfield, 2007). Probably the most
 173 common is the method based on standard penetration testing (SPT). In our study,
 174 due to the lack of SPT data, we use an approach based on the correlation between
 175 penetration resistance and the angle of internal friction for sandy soils (Table 1,
 176 Peck, 1974).

177 Table 1: Relationship between the angle of internal friction and SPT-values (Peck,
 178 1974)

SPT, N-Value	Density of sand	ϕ (degrees)
<4	Very loose	<29
4 – 10	Loose	29 - 30
10 – 30	Medium	30 - 36
30 – 50	Dense	36 - 41
>50	Very dense	>41

179

180 In addition to the friction angle, for modelling the bearing capacity of earthen dikes,
 181 we also consider other geotechnical parameters such as specific weight, porosity
 182 and fines content. Statistical information about the characteristics of dikes used for

183 liquefaction analysis is presented in Table 2. The typical values for the specific
 184 weight and friction angle found in dikes were taken from Vorogushyn et al. (2009)
 185 and the references therein. The fines content values are adapted from a dike at the
 186 Rhine River in the Netherlands (Van Duinen, 2013).

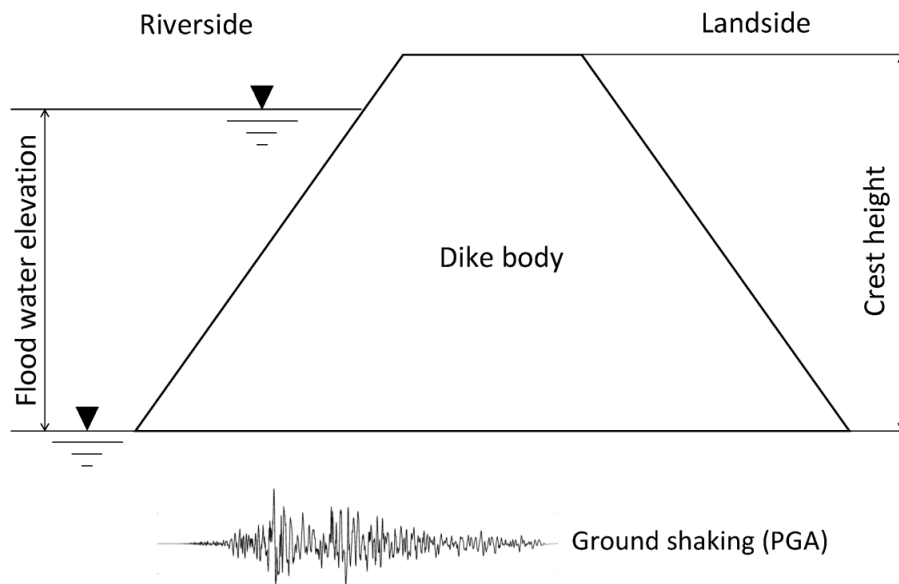
187

188 Table 2: Geotechnical parameters of dikes adopted in this study

Soil properties	Mean	Standard deviation	Minimum	Maximum
Specific weight γ (kN/m ³)	18	1	13	21
Friction angle ϕ	29.2	0.3	20.8	37.6
Fines content FC (%)	5	1	3	11

189

190 The performance of dikes under seismic ground-motion loading is analyzed using a
 191 simplified one-dimensional model assuming that below the water level the soil is in a
 192 saturated state. Hence, the phreatic line within the dike body is assumed to be
 193 horizontal (obviously, this is a conservative assumption that presumes the sufficiently
 194 long duration of the flood water rise or impoundment). A cross-section of the generic
 195 dike model is shown in Fig. 2.



196

197 Figure 2: Generic dike model to illustrate the earthquake-flood-dike interaction

198

199 For the development of dike fragility curves, we assume a generic dike height of 5
 200 meters. When integrated into the dynamic flood-earthquake hazard model, the actual
 201 dike height and corresponding water level need to be taken into account.

202 In the computational algorithm, the material properties of dikes are assumed to be
 203 homogeneously distributed throughout the cross-section of the dike core. However,
 204 they can vary spatially along the river, from one cross-section to another, keeping in
 205 mind the range of existing uncertainties of the geotechnical parameters as specified
 206 in Table 2.

207 For quantifying the liquefaction potential, the values of CSR (reflecting the level of
 208 seismic ground shaking) and CRR (depending on the dike material properties and
 209 the water level) are calculated for all points of the dike cross-section from the crest to
 210 the bottom (with a discretization interval of 5 cm). Once both the CSR and CRR
 211 values have been determined at a certain point under certain load conditions, we can
 212 calculate the factor of safety against liquefaction (FS) employing the relationship
 213 (Seed and Idriss, 1971):

$$214 \quad FS = \frac{CRR}{CSR} \quad (2)$$

215

216 At the points where the loading (CSR) exceeds the resistance (CRR), i.e., the factor
 217 of safety is below 1, one can expect the initiation of liquefaction that can lead to the
 218 functional failure. In this study, we neither analyze the degree of soil deformations
 219 caused by liquefaction nor consider the variety of possible failure states of the
 220 affected structure. Instead, we conservatively assume that the initiation of
 221 liquefaction ($FS \leq 1$) in any point throughout the dike body corresponds to the failure
 222 (loss of function) of the dike.

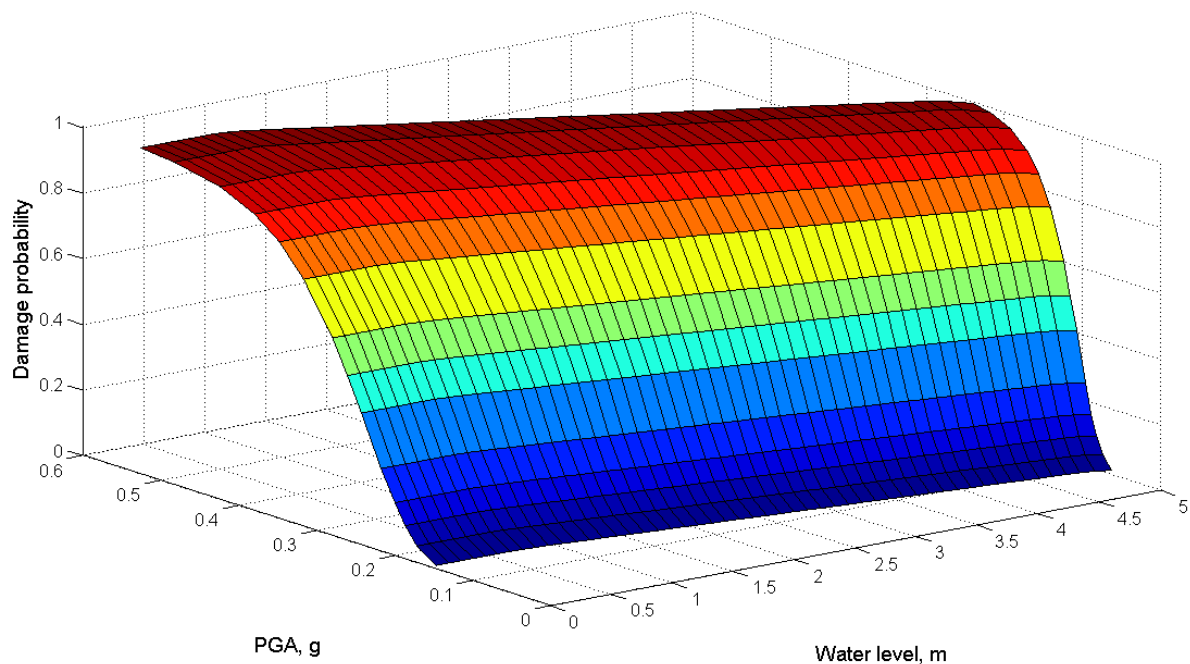
223 Computations of the liquefaction potential are done in a Monte-Carlo simulation
 224 (MCS) considering the variability (uncertainty) of the geotechnical parameters of the
 225 dikes (Table 2). Based on a frequency analysis of the MCS results, dike failure
 226 probabilities are computed for different points of the discretized two-dimensional load
 227 space, considering possible combinations of peak ground acceleration and flood
 228 water level.

229

230 **Fragility surface**

231 In the single hazard fragility analysis, the failure probability is expressed as a
 232 function of single hazard load parameter(s). In a multi-hazard fragility analysis the
 233 response of the structure is described as a function of multiple-hazard load
 234 parameters.. Thus, in our case the calculated fragility results are presented in the
 235 three-dimensional form with seismic and hydraulic load described by peak ground

236 acceleration and water level, respectively (Fig. 3). The fragility surface represents
237 the conditional failure probability given the combination of load.

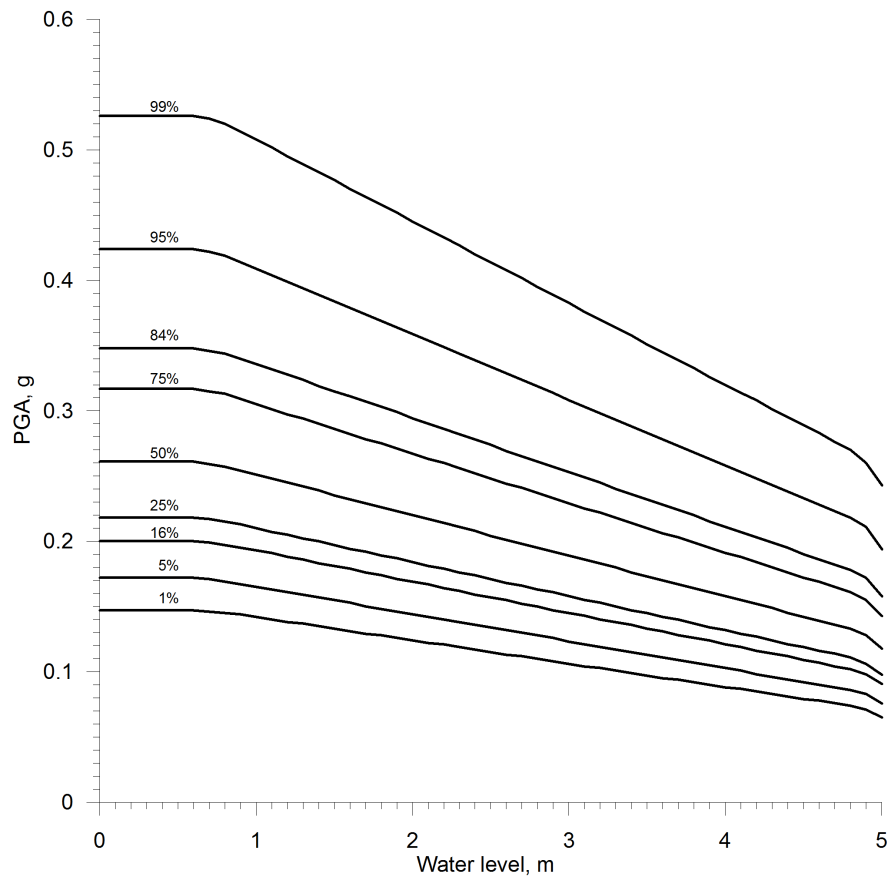


238

239 Figure 3: Multi-hazard fragility surface for liquefaction failure of a dike.

240

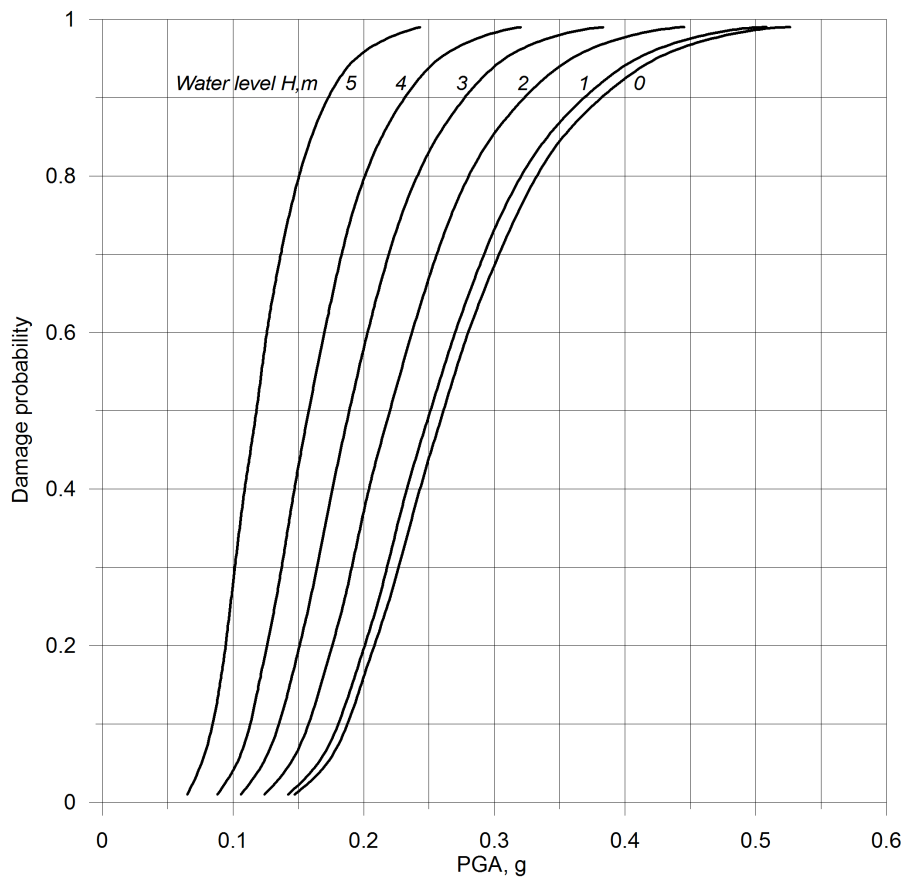
241 The fragility surface can be interpreted as a set of iso-lines corresponding to different
242 percentiles of the calculated distribution of the FS values, as shown in Fig. 4. The
243 presented iso-lines correspond to the occurrence of the limit state ($FS = 1$) and
244 specify the failure probabilities in the two-dimensional space of hazards (in units of
245 PGA and flood water level)..



246

247 Figure 4: Dike failure probability in the PGA and water level space

248 It becomes apparent that liquefaction failure can be initiated already at small water
 249 levels given sufficient earthquake load. On the other turn, a certain degree of
 250 shaking is required for liquefaction failure even at the maximum water levels (Fig. 4).
 251 The estimated PGA threshold ranges from 0.15 g to 0.54 g for the interval from 1 to
 252 99 percentiles. When the flood water rises up to about 0.7 - 0.8 m, it has no visible
 253 effect on the PGA threshold, while further increases in water levels lead to a
 254 considerable shift towards lower PGA values and this change is linear. When the
 255 water level reaches the top of the structure, the threshold PGA values and the
 256 liquefaction occurrence probabilities change significantly. In comparison with the
 257 initial state (water level at the toe of the dike), the PGA threshold values decrease to
 258 between 0.07 - 0.24 g (for the interval from 1 to 99 percentiles). Comparing the two
 259 extreme cases, the liquefaction triggering PGA threshold values decrease more than
 260 half and the spread of the values becomes narrower. Water level is thus a
 261 considerable factor determining the dike core moisture content and liquefaction
 262 failure.



263

264 Figure 5: Fragility functions for earthen dikes for different water levels ranging from
 265 dike toe to assumed crest height.

266

267 The developed dike fragility model may find practical application in regions of low to
 268 moderate seismicity. For the lower PGA values (0.15 - 0.30 g) the contribution of the
 269 effect of impoundment can be more critical than for the higher PGA, when
 270 earthquake ground shaking is sufficiently strong to trigger liquefaction under
 271 conditions without extra-flooding (Fig.5). It should be stressed here that presented
 272 fragility curves represent the conservative estimates due to the assumption of full
 273 saturation of a dike core below the water level. In practice, some time is however
 274 required for the development of the phreatic line. More sophisticated dynamic
 275 models considering the degree of soil saturation can be adapted in future to adjust
 276 failure probability estimates.

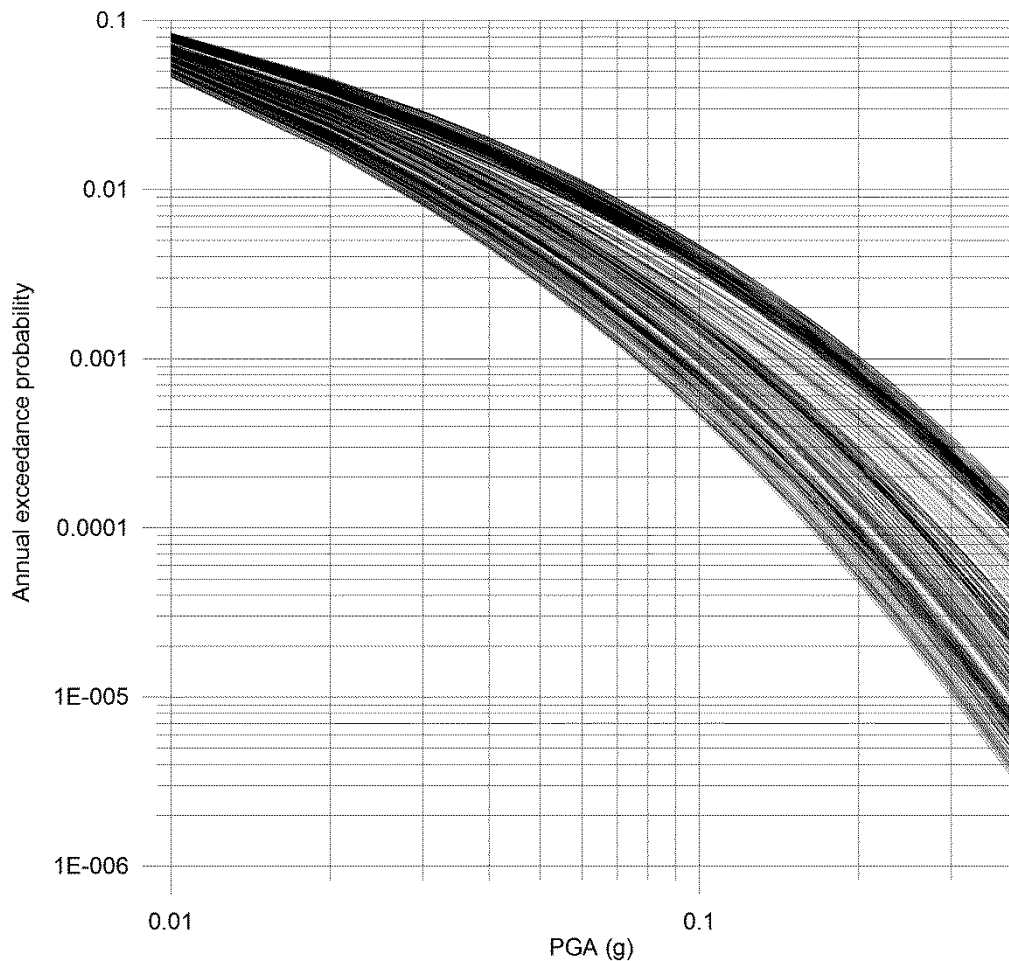
277

278 **Dike failure probability assessment**

279 To estimate the actual failure probability of a dike in the area of interest, the
 280 developed multi-hazard fragility functions should be combined with the probabilistic
 281 hazard estimates of earthquake and flood considering their respective return period
 282 values.

283 The developed fragility curves are intended to be used in a subsequent multi-risk
284 analysis study along the Rhine River reach between Andernach (Rhine-km 613.8)
285 and Düsseldorf (Rhine-km 744.2) considering flood scenarios with return periods
286 between 20 and 1000 years. In particular, the effect of multi-hazard is expected to
287 manifest for flood return periods below the dike design level (200-year return period
288 on the middle Rhine). In the single-type flood hazard analysis only piping failure
289 could possibly impact dikes below design level, whereas multi-hazard consideration
290 would slightly increase the probability of failure if the occurrence of earthquakes and
291 subsequent liquefaction is taken into account. The effect of multi-hazard
292 consideration on total risk is expected to decrease with increasing flood return period
293 beyond design level since dikes would fail (in most cases) due to overtopping
294 anyway.

295 The seismic hazard calculations were implemented for all locations at the center
296 points of dike segments on both sides of the Rhine River reach (Fig. 1). The input
297 data for the seismic hazard analyses were taken in accordance with the regional
298 model of Grünthal et al. (2010). The hazard calculations were implemented using the
299 GEM (Global Earthquake Model) OpenQuake software (Crowley et al., 2011a, b) for
300 soil sites characterized by 300 m/s shear wave (S-wave) velocity in the uppermost
301 30 m, which was assigned considering the results of previous seismological studies
302 in the area (Tyagunov et al., 2006b, Parolai et al., 2007). Note that amongst the
303 waves generated by an earthquake, the S-wave, that are those for which the motion
304 is perpendicular to the direction of wave propagation are expected to determine the
305 largest impact on the building structures. Their variations in the velocity of
306 propagation, accounted in the calculation, are used as a proxy to estimate the spatial
307 differences in the amplitude of shaking. The set of calculated seismic hazard curves
308 in terms of PGA characterize the range of probable level of ground shaking for the
309 different dike locations is shown in Fig. 6. In total, 339 dike sections are analysed:
310 157 of them are on the left side and 182 on the right side of the river.



311

312 Figure 6: Seismic hazard (mean) curves for the locations of the dikes along the
 313 Rhine River. Each curve corresponds to one dike segment.

314 The calculated PGA values vary in space for different points along the river stretch
 315 and the level of ground shaking depends on the return period of interest. Thus, for
 316 the level of exceedance probability of 10% in 50 years, which is the common
 317 standard in the practice of earthquake engineering and corresponds to an average
 318 return period of 475 years, the PGA estimates vary over a range of about 0.06 – 0.15
 319 g. For a shorter return period of 100 years, PGA varies in the range of about 0.03 –
 320 0.06 g, whereas for a longer return period of 1000 years the range is about 0.08 –
 321 0.20 g. Note, however, that for the return periods longer than 1000 years, even
 322 higher levels of ground shaking are probable in the area and such low probability
 323 phenomena cannot be ruled out.

324 The spread in the calculated PGA values is not very large, because the course of the
 325 Rhine River and corresponding dikes closely follows the shape of the seismic hazard
 326 zones around Cologne (Grünthal et al., 1998, DIN 4149, 2005). Therefore the
 327 seismic hazard distribution in the area under study (Fig. 1) appears rather uniform.

328 On the basis of the obtained results and referring to the liquefaction susceptibility
 329 categorization for different soil types (Youd and Perkins, 1978, HAZUS-MH, 2003),

330 one can make a qualitative conclusion that in this area, there is a risk of dike
 331 damage due to liquefaction induced by seismic ground shaking. According to
 332 observations from past earthquakes (Sasaki et al., 2004) seismic damage to river
 333 dikes can be triggered by PGA of 0.16 g or higher. There is even evidence that the
 334 PGA threshold for liquefaction occurrence can be even less than 0.10 g (Santucci de
 335 Magistries et al., 2013, Quigley et al., 2013).

336 The actual dike failure probabilities can be quantified by considering the probabilities
 337 of occurrence of the earthquake ground shaking level and flood return periods at
 338 different dike locations combined with the presented fragility curves. The
 339 simultaneous occurrence of a flood and an earthquake should be assumed. The
 340 typical duration of a flood wave of 30 days is considered for the Rhine. It is assumed
 341 that no dike repair actions are undertaken in this period, which may affect the
 342 probability of failure. Thus, the earthquake probability is computed for this period to
 343 be combined in the following expression to determine the actual failure probability

344

$$345 \quad P(F) = \iint P(F|S_i^{30}, W_j) * P(S_i^{30}) * P(W_j) dSdW, \quad (3)$$

346

347 where $P(F|S_i^{30}, W_j)$ is the conditional failure probability given the combination of
 348 the seismic ground shaking S_i^{30} within a time window of 30 days and the water level
 349 W_j ;

350 $P(S_i^{30})$ is the probability of occurrence of the seismic input S (peak ground
 351 acceleration) of the level i within a time window of 30 days;

352 $P(W_j)$ is the probability that the water level W corresponds to the level j .

353 The first factor in the integral represents the conditional failure probabilities, which
 354 can be obtained from the multi-hazard fragility surface (Fig. 3), while the second and
 355 third ones represent probabilistic estimates of the seismic (PGA level) and flood
 356 hazard (water level) at the dike locations and can be obtained from the
 357 corresponding hazard curves.

358 For the situation without flooding by combining the seismic hazard curves (Fig. 6)
 359 with the fragility curve corresponding to the water level of 0 m (Fig. 5), the
 360 earthquake-triggered liquefaction may occur at some of the considered dike
 361 locations though the probability is not very high. The probability varies in this case
 362 within the range of $1 - 4 \cdot 10^{-5}$ per year.

363 The current design criteria of fluvial dikes take into account only flood hazard and do
 364 not consider potential multi-hazard impact. Therefore, in case of probable temporal
 365 coincidence of flooding and strong earthquakes, dike protection structures may fail

366 due to liquefaction at flood return periods below the design level. This may lead to
367 perplexity and negatively affect population, infrastructure, and flood response,
368 requiring emergency actions.

369 A comprehensive quantitative risk analysis considering the joint probability of seismic
370 and flood events and their interactions in time and space requires continuous
371 hydraulic model and multi-hazard integration. This goes beyond the scope of
372 presented research. Here, for the illustration purpose, we present an example for
373 estimation of the failure probability for a specific dike section.

374 For a left-side dike section at Rhine-km 668 near the town Wesseling (south to the
375 city of Cologne, Fig.1), the average maximum water levels were estimated for three
376 return periods 200, 500 and 1000 years, using a dynamic probabilistic-deterministic
377 coupled 1D-2D model (Vorogushyn et al., 2010) setup for the study area at the
378 Rhine River within the EU-FP7 MATRIX project (Garcia-Aristizabal and Marzocchi,
379 2013). The hydraulic model uses the flow records at gauge Andernach (Rhine-km
380 613.8) for estimation of hydrographs and corresponding return periods. Hydrographs
381 are then routed with a coupled 1D-2D model considering dike breaches and
382 associated inundation. The estimated water levels at the selected location are: for
383 the 200-year return period ($p=0.005$ per year) 50.38 m asl (above sea level); for 500-
384 year ($p=0.002$) and 1000-year ($p=0.001$) 50.49 m and 50.52 m asl, correspondingly.

385 Assuming the height of the dike of 5 metres at the selected location, the dike would
386 be impounded by 4.50 metres during a 200-year flood event. Correspondingly, the
387 estimated impoundment level would reach 4.61 m for the 500-year and 4.64 m for
388 the 1000-year flood scenarios. The small difference between the calculated
389 estimates can be explained, in particular, by the used model, which considers dike
390 breaches upstream, i.e. the water level at one dike location depends on performance
391 of other dike sections (e.g., if one of the upstream dikes fails, the water outflow
392 would reduce the flood loads on the other dike sections).

393 Combining the flood hazard estimates with seismic hazard curves and fragility
394 function for the point of interest, the probability of liquefaction at Wesseling without
395 flooding is about $3.9 \cdot 10^{-5}$ per year. Applying Eq. 3, we obtain for the 200-year flood
396 scenario the liquefaction failure probability of $1 \cdot 10^{-6}$ per year, for the 500-year flood –
397 about $4.1 \cdot 10^{-7}$ per year and for the 1000-year flood – about $2.1 \cdot 10^{-7}$ per year. All
398 these return period scenarios contribute to the total risk value. Consequently, it is
399 expected that the multi-hazard interaction scenarios essentially increase the total risk
400 level in comparison with the estimated single hazard risk level though the combined
401 probabilities of earthquake and floods are very small.

402 Nevertheless, dike failures due to liquefaction in case of a multi-hazard impact bears
403 the potential of surprise and malign consequences, which should be considered in a
404 comprehensive risk assessment (Merz et al., 2015). In particular, under hydraulic
405 load below the (hydraulic) design level (< 200 -year return period at the German

406 Rhine reach), dikes might be considered predominantly safe in a single-type hazard
407 analysis, whereas the occurrence of liquefaction would dramatically change flood
408 inundation patterns and loss distribution. Though not necessarily extreme, but still
409 significantly strong floods and 'unexpected' dike failures in combination may still
410 harmfully affect the densely populated areas with high asset concentration such as
411 floodplains along the Rhine. Hence, a quantitative multi-risk analysis is advocated in
412 earthquake and flood prone areas considering the effect of dike liquefaction despite
413 a relatively small probability of the joint occurrence of both perils.

414

415 **Conclusions**

416 A methodology for multi-hazard fragility and failure probability analyses of fluvial
417 dikes in earthquake and flood prone areas is presented. The system of flood
418 protection dikes along the Rhine River in the area around Cologne is analysed,
419 considering their possible failures due to liquefaction induced by seismic ground
420 shaking in combination with flooding. We conservatively assume the initiation of
421 liquefaction at any point throughout the dike body leads to the dike failure.

422 The failure probability is presented as a three-dimensional fragility surface as a
423 function of both earthquake ground shaking (PGA) and flood water level
424 (impoundment of the dike). Quantitative fragility analysis shows that a rise in flood
425 water level reduces the liquefaction triggering PGA threshold due to high moisture
426 content in the dike core.

427 When considering earthquake and flood hazard and the developed fragility curves,
428 the non-zero liquefaction probability for an exemplary dike location becomes evident.
429 Though the probability of joint occurrence of both perils is rather low, we argue that
430 such incidents bear a high potential of surprise with substantial negative
431 consequences. The latter can be, however, avoided by multi-risk considerations and
432 awareness at civil protection authorities and within the public.

433 The developed fragility curves for liquefaction will be used for comprehensive multi-
434 risk assessment study along the Rhine River in a subsequent work. This will take
435 into the interaction of earthquake and flood hazards into account, dynamic
436 inundation effects and damage modelling.

437

438 **Acknowledgements**

439 The presented research has received funding from the European Community's
440 Seventh Framework Programme [FP7/2007-2013] under grant agreement n°
441 265138.

442

443 **References**

- 444 Allsop, W., Kortenhaus, A., Morris, M., Buijs, F., Hassan, R., Young, M., Doorn, N.,
 445 van der Meer, J., van Gelder, P., Dyer, M., Redaelli, M., Uily, S., Visser, P., Bettess,
 446 R., Lesniewska, D., and ter Horst, W.: Failure mechanisms for flood defence
 447 structures, FLOODSite Project Report T04 06 01, FLOODSite Consortium, 2007.
 448 203 p.
- 449 Apel, H., Thieken, A., Merz, B., and Blöschl, G. (2004): Flood risk assessment and
 450 associated uncertainty, *Nat. Hazards Earth Syst. Sci.*, 4, 295-308.
- 451 Armbruster-Veneti, H. (1999): Über das Versagen von Erddämmen,
 452 *Wasserwirtschaft*, 89, 504–511.
- 453 Athanasopoulos-Zekkos, A. and Seed R. B. (2013): Seismic Slope Stability of
 454 Earthen Levees. *Proc. of the 18th International Conference on Soil Mechanics and*
 455 *Geotechnical Engineering, Paris 2013*, 1423-1426.
- 456 Briaud, J., Chen, H., Govindasamy, A., and Storesund, R. (2008): Levee Erosion by
 457 Overtopping in New Orleans during the Katrina Hurricane. *J. Geotech. Geoenviron.*
 458 *Eng.* 134, SPECIAL ISSUE: Performance of Geo-Systems during Hurricane Katrina,
 459 618–632.
- 460 Crowley, H., Monelli, D., Pagani, M., Silva, V., and Weatherill, G.: OpenQuake
 461 User's Manual, www.globalquakemodel.org (last access: 30 May 2012), 2011a.
- 462 Crowley, H., Monelli, D., Pagani, M., Silva, V., and Weatherill, G.: OpenQuake Book,
 463 www.globalquakemodel.org (last access: 30 May 2012), 2011b.
- 464 DIN 4149, 2005. Bauten in deutschen Erdbebengebieten - Lastannahmen,
 465 Bemessung und Ausführung üblicher Hochbauten.
- 466 Fink, A., Ulbrich, U. and Engel, H. (1996): Aspects of the January 1995 flood in
 467 Germany, *Weather*, 51, 34-39.
- 468 Fleming, K., Parolai, S., Garcia-Aristizabal, A., Tyagunov, S., Vorogushyn,
 469 S., Kreibich, H., Mahlke, H. (2016): Harmonizing and comparing single-type natural
 470 hazard risk estimations. - *Annals of Geophysics*, 59, 2.
- 471 Foster, M., Fell, R. and Spannagle, M. (2000): The statistics of embankment dam
 472 failures and accidents, *Canadian Geotechnical Journal*, Vol. 37, No. 5, National
 473 Research Council Canada, Ottawa, 1000–1024, ISSN 0008-3674.
- 474 Garcia-Aristizabal, A. and Marzocchi, W. (2013): Deliverable: D3.3: Scenarios of
 475 cascade events, EU-FP7 Project MATRIX (New methodologies for multi-hazard and
 476 multi-risk assessment methods for Europe), URL:
 477 <http://matrix.gpi.kit.edu/downloads/MATRIX-D3.03.pdf>.

- 478 Grünthal, G., Mayer-Rosa, D., and Lenhardt, W. A. (1998): Abschätzung der
479 Erdbebengefährdung für die D-A-CH-Staaten – Deutschland, Österreich, Schweiz.
480 Bautechnik, 10, 753–767, 1998.
- 481 Grünthal, G., Thieken, A.H., Schwarz, J., Radtke, K.S., Smolka, A. and Merz, B.
482 (2006): Comparative risk assessments for the city of Cologne – Storms, Floods,
483 Earthquakes, Natural Hazards, 38, 21-44. doi:10.1007/s11069-005-8598-0
- 484 Grünthal, G., Wahlström, R., and Stromeyer, D. (2009): The unified catalogue of
485 earthquakes in central, northern, and northwestern Europe (CENEC) – updated and
486 expanded to the last millennium, J. Seismol, 13, 517–541, 2009.
- 487 Grünthal, G., Arvidsson, R., and Bosse, Ch. (2010): Earthquake Model for the
488 European-Mediterranean Region for the Purpose of GEM1, Scientific Technical
489 Report SRT10/04, GFZ, 36, 2010.
- 490 HAZUS-MH (2003): Multi-hazard loss estimation methodology, HAZUS-MH MR4
491 Technical Manual, Federal Emergency Management Agency, Washington DC, 2003.
- 492 Hofherr, T. and Kunz, M. (2010): Extreme wind climatology of winter storms in
493 Germany. Climate Research, 41, 105-123.
- 494 Huang, W. C., Weng, M. C., Chen, R. K. (2014): Levee failure mechanisms during
495 the extreme rainfall event: a case study in Southern Taiwan, Natural Hazards,
496 January 2014, Volume 70, Issue 2, 1287-1307. doi:10.1007/s11069-013-0874-9
- 497 Idriss, I. M. and Boulanger, R. W. (2008): Soil Liquefaction During Earthquakes.
498 EERI MNO-12, 2008.
- 499 KATARISK (2003): Disasters and Emergencies in Switzerland. Risk assessment
500 from a civil protection perspective. Federal Office for Civil Protection (Switzerland),
501 2003, 82 p.
- 502 Kishida, T., Boulanger, R. W., Abrahamson, N. A., Driller, M. D., and Wehling, T. M.,
503 (2009): Seismic response of levees in the Sacramento-San Joaquin Delta,
504 Earthquake Spectra, 25 (3), 557–582.
- 505 Kramer, S. L. (1996): Geotechnical Earthquake Engineering, Prentice Hall, New
506 Jersey, 1996. 653 p.
- 507 Kramer, S. and Mayfield, R. (2007): Return Period of Soil Liquefaction. J. Geotech.
508 Geoenviron. Eng., 133(7), 802–813.
- 509 Krzhizhanovskaya, V.V. Shirshov, G.S. Melnikova, N.B. Belleman, R.G. Rusadi, F.I.
510 Broekhuijsen, B.J. Gouldby, B.P. Lhomme, J. Balis, B. Bubak M. (2011): Flood early
511 warning system: design, implementation and computational modules. Procedia
512 Computer Science, 4, 106-115, DOI: 10.1016/j.procs.2011.04.012

- 513 Marcuson, W.F.III, Hynes, M.E. and Franklin, A.G. (2007): Seismic Design and
514 Analysis of Embankment Dams: The State of Practice. Proc. of the 4th Civil
515 Engineering Conference in the Asian Region. June 25-28, 2007, Taipei.
- 516 Marzocchi, W., Garcia-Aristizabal, A., Gasparini, P., Mastellone, M.L., Di Ruocco, A.
517 (2012): Basic principles of multi-risk assessment: a case study in Italy. Nat Hazards.
518 doi:10.1007/s11069-012-0092-x
- 519 Merz, B., Vorogushyn, S., Lall, U., Viglione, A., Blöschl, G. (2015): Charting unknown
520 waters - On the role of surprise in flood risk assessment and management. - Water
521 Resources Research, 51, 8, 6399-6416. doi: 10.1002/2015WR017464
- 522 Mignan, A., Wiemer, S., and Giardini, D. (2014): The quantification of low-probability-
523 high-consequences events: part I. A generic multi-risk approach, Nat. Hazards,
524 doi:10.1007/s11069-014-1178-4
- 525 Nagy, L. (2012): Statistical evaluation of historical dike failure mechanism. Riscuri ul
526 Catastrofe, XI, 11 (2), 2012, 7-20.
- 527 Newmark, N. M. (1965): Effects of Earthquakes on Dams and Embankments,
528 Geotechnique, 15 (2), 139-160.
- 529 Ozkan (1998): A review of consideration on seismic safety of embankments and
530 earth and rock-fill dams. Soil Dynamics and Earthquake Engineering, 17, 439-458.
- 531 Parolai, S., Grünthal, G., Wahlström, R. (2007): Site-specific response spectra from
532 the combination of microzonation with probabilistic seismic hazard assessment — an
533 example for the Cologne (Germany) area. Soil Dynamics and Earthquake
534 Engineering, 27, 1, 49-59.
- 535 Peck, R. B., Hanson, W. E., and Thornburn, T. H. (1974): Foundation Engineering.
536 John Wiley & Sons, New York.
- 537 Quigley, M.C., Bastin S., Bradley B.A. (2013): Recurrent liquefaction in Christchurch,
538 New Zealand, during the Canterbury earthquake sequence. Geology, 41 (2013),
539 419–422.
- 540 Rosidi D. (2007): Seismic Risk Assessment of Levees. Civil Engineering Dimension,
541 Vol.9, No.2; 57-63.
- 542 Sasaki, Y., Kano, S., and Matsuo, O. (2004): Research and Practices on Remedial
543 Measures for River Dikes against Soil Liquefaction. Journal of Japan Association for
544 Earthquake Engineering, Vol.4, No.3 (Special Issue), 2004, 312-335.
- 545 Santucci de Magistris, F., Lanzano, G., Forte, G., Fabbrocino, G. (2013): A
546 database for PGA threshold in liquefaction occurrence. Soil Dynamics and
547 Earthquake Engineering, Volume 54, November 2013, 17-19.

- 548 Schweckendiek, T., Vrouwenvelder, A., Calle, E.O.F. (2014): Updating piping
549 reliability with field performance observations. *Structural Safety*, 47, 13-23.
- 550 Seed, H. B., and Idriss, I. M. (1971): Simplified procedure for evaluating soil
551 liquefaction potential. *J. Geotech. Engrg. Div., ASCE*, 97(9), 1249–1273.
- 552 Sellmeijer, J. B., (1989): On the mechanism of piping under impervious structures.
553 Ph.D. thesis, Delft University of Technology, The Netherlands.
- 554 Selva, J. (2013): Long-term multi-risk assessment: statistical treatment of interaction
555 among risks. *Natural Hazards*, 67(2),701-722. doi:10.1007/s11069-013-0599-9
- 556 Singh, R. and Roy, D. (2009): Estimation of Earthquake-Induced Crest Settlements
557 of Embankments. *American J. of Engineering and Applied Sciences* 2 (3): 515-525.
- 558 Tyagunov, S., Grünthal, G., Wahlström, R., Stempniewski, L., Zschau, J. (2006a):
559 Seismic risk mapping for Germany. *Natural Hazards and Earth System Sciences*
560 (NHESS), 6, 4, 573-586.
- 561 Tyagunov, S., Hollnack, D., Wenzel, F. (2006b): Engineering-Seismological Analysis
562 of Site Effects in the Area of Cologne. *Natural Hazards*, 38, 2006, 199-214.
- 563 Van Baars, S., and Van Kempen, I. M. (2009): The Causes and Mechanisms of
564 Historical Dike Failures in the Netherlands. Official Publication of the European
565 Water Association (EWA). ISSN1994-8549
- 566 Van Duinen (2013): Data of Spui dike at Oud-Beijerland, The Netherlands, personal
567 communication, 18.01.2013.
- 568 Vorogushyn, S., Merz, B., Apel, H. (2009): Development of dike fragility curves for
569 piping and micro-instability breach mechanisms. *Natural Hazards and Earth System*
570 *Sciences* 9, 1383–1401.
- 571 Vorogushyn, S., Merz, B., Lindenschmidt, K.-E., and Apel H. (2010): A new
572 methodology for flood hazard assessment considering dike breaches, *Water*
573 *Resources Research*, 46 (8), 2010, doi:10.1029/2009WR008475
- 574 Vrouwenvelder, A. C. W. M., Wubs, A. J. (1985): Een probabilistisch dijkontwerp (A
575 probabilistic dyke design). Technical Report B-85-64/64.3.0873, TNO-IBBC, Delft,
576 The Netherlands, (in Dutch).
- 577 Wang, M., Chen, G., and lai, S. (2013): Seismic performances of dyke on liquefiable
578 soils, *Journal of Rock Mechanics and Geotechnical Engineering* 01/2013; 5 (4), 294–
579 305.
- 580 Wolff, T. F. (2008): Reliability of levee systems. In Phoon, K. K., editor, *Reliability-*
581 *based design in Geotechnical Engineering*, chapter 12, pages 449–496. Taylor &
582 Francis, London and New York.

- 583 Youd, T. L. and Perkins, D. M. (1978): Mapping liquefaction-induced ground failure
584 potential, *J. Geotech. Eng. Division*, 104, 443–446.
- 585 Youd, T., Idriss, I., Andrus, R., Arango, I., Castro, G., Christian, J., Dobry, R., Finn,
586 W., Harder, L., Jr., Hynes, M., Ishihara, K., Koester, J., Liao, S., Marcuson, W., III,
587 Martin, G., Mitchell, J., Moriwaki, Y., Power, M., Robertson, P., Seed, R., and
588 Stokoe, K., II (2001): Liquefaction Resistance of Soils: Summary Report from the
589 1996 NCEER and 1998 NCEER/NSF Workshops on Evaluation of Liquefaction
590 Resistance of Soils. *J. Geotech. Geoenviron. Eng.*, 127 (10), 817–833.